Physics – Uspekhi **68** (4) 393 – 400 (2025)

INSTRUMENTS AND METHODS OF INVESTIGATION

PACS numbers: 61.05.C – , 61.50.Ah, 78.70.Ck, 78.70.Dm

ON THE 270th ANNIVERSARY OF M.V. LOMONOSOV MOSCOW STATE UNIVERSITY (MSU)

Interference phenomena in X-ray diffraction spectroscopy

E.N. Ovchinnikova, A.P. Oreshko, V.E. Dmitrienko

DOI: https://doi.org/10.3367/UFNe.2025.03.039876

Contents

Abstract. **We provide a review of recent research concerning the interference of several scattering channels of synchrotron radiation with wavelengths near the atomic absorption edges in crystals. The experimental conditions and theoretical approaches that yield the possibility of separating the contributions to the intensity of Bragg reflections from different types of scattering are considered, specific examples of studies are given, and the role of interference is discussed. It is shown that the resultant data yield unique information about different types of ordering (structural, charge, magnetic, etc.) at the atomic level and their dynamic behavior under external influences.**

Keywords: X-ray radiation, synchrotron radiation, resonant diffraction, interference, forbidden reflections

1. Introduction

Modern technical progress calls for the development of a wide range of materials with controlled functional properties that depend on different types of ordering (structural, charge, magnetic, etc.). In order to control such properties, it is necessary to have tools for obtaining the most complete information about ordering under different external conditions.

Among the traditional methods for studying structural and electronic ordering are X-ray diffraction methods [1]. Such methods provide information averaged over a group of scattering atoms. The need to obtain local nonaveraged data invited the development of resonance X-ray methods. These methods analyze the absorption and scattering spectra of radiation with an energy close to the absorption edges of any atom of the substance under study [2–7], which makes it possible to obtain new unique information about different types of ordering of functional materials and their dynamic behavior under external influence [7–9].

The practical implementation of X-ray resonance methods is inextricably linked to the use of synchrotron radiation (SR) sources, which have a wide continuous spectrum ranging from the infrared to the X-ray region and the ability to 'tune' to resonance studies of strictly defined chemical elements. Due to the simple experimental setup [8], resonance methods have historically been more extensively used in absorption (transmission) geometry, but recent years have seen increasing interest in elastic scattering geometry: diffraction spectroscopy, where a study is made of the spectral composition of Bragg diffraction reflections. Using X-ray diffraction spectroscopy, charge, magnetic, and orbital ordering in crystals of different symmetry [10–12] has been studied, including elements from virtually the entire periodic table, from carbon to actinides [13, 14].

As is well known, in the case of coherent elastic scattering of SR in crystals, regular extinctions are observed in the resulting diffraction pattern, i.e., the absence of certain diffraction peaks (reflections) due to the destructive interference of waves scattered by crystallographically equivalent atoms. The set of such extinctions is determined by the space group of the crystal [15], and the conditions limiting the possible diffraction reflections (extinction rules) are obtained under the assumption that atoms in equivalent positions scatter SR once and isotropically [16], regardless of the orientation of their local environment. Actually, due to interaction with each other, atoms in equivalent crystallographic positions may be nonequivalent in terms of their interaction with SR, i.e., anisotropy of scattering arises [17], and this anisotropy is associated precisely with the local orientation of the atomic environment, with the direction of magnetic and multipole moments, etc. A consistent description of the anisotropy of SR scattering

E.N. Ovchinnikova [(1,*)], **A.P. Oreshko** [(1)], **V.E. Dmitrienko** [(2)]
[(1)] Lomonosov Moscow State University, Faculty of Physics, Leninskie gory 1, str. 2, 119991 Moscow, Russian Federation
[(2)] Shubnikov Institute of Crystallography of the Kurchatov Complex Crystallography and Photonics of the NRC Kurchatov Institute, Leninskii prosp. 59, 119333 Moscow, Russian Federation
E-mail: [(*)] OvchinnikovaEN@my.msu.ru

Received 20 February 2025, revised 2 March 2025
Uspekhi Fizicheskikh Nauk **195** (4) 416 – 424 (2025)
Translated by E.N. Ragozin

by atoms of a substance relies on quantum-mechanical theory and requires knowledge of the atomic and crystalline wave functions of electrons [18–23]. The physical causes of the anisotropy consist in the distortion of the atomic electron wave functions by the crystalline field and spin-orbit interaction [24, 25] and are caused, for example, by the asymmetry [26, 27] and local chirality [28, 29] of the environment of the scattering atom or thermal vibrations [30]. To describe the anisotropic properties of synchrotron radiation scattering by atoms, use is made of tensor corrections to the X-ray polarizability of the medium, whereas the main (potential) part of the polarizability is isotropic.

In the formation of the spectra of allowed diffraction reflections, the main role is played by strong nonresonant potential (Thomson) isotropic scattering of SR by the electron density of the atom, with the inclusion of the scalar dispersion corrections, while the resonance effects of scattering anisotropy are weakly pronounced [16, 23, 24]. To study such subtle effects, advantage is taken of the spectra of resonance forbidden Bragg reflections, which arise at the site of regular extinctions, where the extinction rules suppress the main isotropic channel of SR scattering by atoms [31, 32] (reviews of early studies are given in Refs [24, 33]).

In some cases, forbidden reflections can be caused by the simultaneous presence of several anisotropic factors [34]. Then, one more unique feature appears in their spectral dependences: the interference nature of resonant scattering. Specifically, observation of the interference of dipole-quadrupole and thermally induced resonant scattering in germanium crystals, wurtzites, and ferroelectrics with a KDP-type structure made it possible to determine the frequencies of phonon modes, the correlation functions of atomic displacements, and the defect activation energies [35–37]. The interference of nonresonant magnetic and resonant quadrupole SR scattering made it possible to reveal a change of sign of the Dzyaloshinskii–Moriya interaction in a number of isostructural compounds of transition metals [38–42]. The interference of resonant and nonresonant SR scattering channels, despite the fact that the amplitude of anisotropic resonant scattering is usually several orders of magnitude lower than the amplitude of isotropic scattering, was used in Ref. [43] to study the formation of a polar phase in nonpolar strontium titanate under the action of an external electric field. In turn, the difference among the polarization characteristics of SR scattering channels, in principle, permits separating resonant scattering from strong scattering by electron density [44], which is especially important in the study of those functional materials in which there are no diffraction reflections forbidden by symmetry. A separate issue is the existence of additional 'cross' terms [45] in scattering amplitudes, but they have not yet been experimentally detected due to their smallness.

Considered in this paper are several recent examples of the existence and practical use of interference of different SR scattering channels in crystals, which are interesting from a physical point of view.

2. Intensity of Bragg reflections with inclusion of resonance contributions

In X-ray diffraction methods for condensed media research, the main quantity characterizing the interaction of radiation with matter is the atomic scattering amplitude (atomic scattering factor), which determines the amplitude of the wave scattered by one atom of matter [16]. With the inclusion of all components arising both near and far from the absorption edges, this quantity is of the form [45, 23]

$$f_{ij}(E) = f^{(\mathrm{nr})}\delta_{ij} + f_{ij}^{(\mathrm{magn})} + f_{ij}^{(\mathrm{an})}(E)\,, \tag{1}$$

where the nonresonant part of the atomic scattering amplitude $f^{(\mathrm{nr})} = (f_0 + f_0'(E) + \mathrm{i}f_0''(E))$, f_0 is the amplitude of potential scattering, f_0' and f_0'' are the real and imaginary parts of the correction, which include the isotropic part of the dispersion and absorption effects ($\sim 10^{-1} f_0$), $f_{ij}^{(\mathrm{magn})}$ ($\sim 10^{-2} - 10^{-3} f_0$) is the amplitude of magnetic nonresonant scattering, and $f_{ij}^{(\mathrm{an})}(E)$ ($\sim 10^{-1} - 10^{-2} f_0$) describes anisotropic scattering.

In view of magnetic and anisotropic corrections to the atomic scattering amplitude, the amplitude of diffraction Bragg reflections with indices $\mathbf{H} = (h, k, l)$ is described by the tensor structural amplitude

$$F_{ij}(\mathbf{H}) = \sum_m f_{ij}^m \exp\{\mathrm{i}\mathbf{H}\mathbf{r}^m\}\,, \tag{2}$$

where $\mathbf{r}^m$ is the coordinate of the mth atom in the unit cell, with the summation performed over all such atoms.

In the kinematic approximation of diffraction theory, the intensity of diffraction Bragg reflections, considering the anisotropy of absorption and scattering of SR, is defined by the expression [46]

$$I(\mathbf{H}) \sim \int_0^\infty \left|\mathbf{A}^+ \hat{T}_{\mathrm{sc}}\, \hat{F} \hat{T}_{\mathrm{in}}\, \mathbf{P}\right|^2 \mathrm{d}z\,, \tag{3}$$

where $\mathbf{P}$ and $\mathbf{A}^+$ define the polarization states of the incident and scattered radiation, respectively, $\hat{F}$ is the matrix of the structural amplitude in polarization indices, $\hat{T}_{\mathrm{in}}$ and $\hat{T}_{\mathrm{sc}}$ are the radiation propagation matrices in the crystal in the direction of the incident (in) and diffracted (elastically scattered) (sc) waves, integration is performed along the normal deep into the crystal surface, which is taken as semi-infinite in the Bragg diffraction geometry, and the '+' sign denotes complex transposition. The explicit form of the radiation propagation matrices $\hat{T}_{\mathrm{in}}(\hat{T}_{\mathrm{sc}})$ is related to the symmetry of the structure under study and the type of resonant transition, and is given in Refs [47, 48].

In the presence of several different physical factors responsible for the emergence of scattering anisotropy, the matrix of the structural amplitude, accurate to quadrupole-quadrupole terms of the expansion of the atomic scattering factor, has the form [34]

$$F_{\alpha\beta} = \sum_{m,p} e_\alpha^{(\mathrm{in})} e_\beta^{(\mathrm{sc})*} \left[f^{(\mathrm{nr})m} + D_{\alpha\beta}^{m,p} + \mathrm{i}\left(k_\gamma^{(\mathrm{in})} I_{\alpha\beta\gamma}^{m,p} - k_\gamma^{(\mathrm{sc})} I_{\beta\alpha\gamma}^{m,p}\right) + k_\gamma^{(\mathrm{in})} k_\delta^{(\mathrm{sc})} Q_{\alpha\beta\gamma\delta}^{m,p} \right] \exp\{\mathrm{i}\mathbf{H}\mathbf{r}^m\}\,, \tag{4}$$

where m is the number of the atom in the unit cell, $\mathbf{k}^{(\mathrm{in}),(\mathrm{sc})}$ and $\mathbf{e}^{(\mathrm{in}),(\mathrm{sc})}$ are the wave vectors and polarization vectors of the incident and scattered radiation, α and β denote two orthogonal polarizations, and the summation is performed over the repeating indices γ and δ. For the dipole-dipole, dipole-quadrupole, and quadrupole-quadrupole components of the anisotropic part of the mth atomic scattering factor generated by the pth physical cause, we employ the notation $D_{\alpha\beta}^{m,p}$, $I_{\alpha\beta\gamma}^{m,p}$, and $Q_{\alpha\beta\gamma\delta}^{m,p}$, respectively [23, 49]. These tensor quantities are generally complex, and they depend resonantly on the energy of the incident radiation.

So, although the structural amplitude is represented by a linear combination of different contributions, the intensity of

diffraction reflections, proportional to its modulus squared, is no longer equal to the sum of the intensities corresponding to each scattering channel separately. Specifically, because all secondary waves resulting from various physical processes are coherent [47], they interfere, and in the expression for the intensity of diffraction Bragg reflections interference terms arise, which may greatly change both the intensity and the polarization properties of the reflections.

Despite the fact that resonant diffraction Bragg reflections have been repeatedly observed, the interpretation of the resultant experimental data is a very difficult task, since it requires knowledge of the wave functions of the excited states of the crystal atoms. So far, there are no methods for solving the inverse problem, and for solving the direct problem, i.e., modeling the intensity of diffraction reflections, the programs that enjoy the widest application are FEFF9 [50], WIEN2k [51], and FDMNES [52].

3. Several resonance channels of X-ray scattering

When studying the spectra of forbidden diffraction reflections, the problem arises of finding conditions whereby not only allowed reflections are absent, but so is the indirect multiwave excitation of forbidden reflections via allowed ones [53]. By tuning out from nonresonant scattering channels [54], one may discover, however, that the spectra of forbidden reflections sometimes cannot be described by only one type of resonant scattering.

Interference phenomena occur when several physical mechanisms contribute to the same diffraction reflection. To date, quite extensive studies have been done on structures in which several types of atomic ordering are present, while resonant scattering by different substructures makes contributions to different diffraction reflections. For instance, in the $La_{0.5}Sr_{1.5}MnO_4$ crystal, charge, magnetic, and orbital ordering on manganese atoms gives rise to different types of diffraction reflection satellites due to the difference among the periods of the corresponding substructures [10, 11]. There are also cases in which additional reflections are integers, but their observation conditions do not coincide; an example is the GdB_4 crystal, where dipole-dipole and magnetic resonant scattering are present, but the magnetic contribution is absent above the Neel temperature [55]. In all these cases, interference phenomena due to the simultaneous presence of several scattering channels do not manifest themselves.

One of the striking examples of the simultaneous existence of several channels of resonant SR scattering and the possibility of their separation is the (006) reflection in germanium crystals. The $Fd\bar{3}m$ space symmetry group of germanium prohibits the existence $(0kl)$ of diffraction reflections, where $k + l = 4n + 2$. Furthermore, since the symmetry of the equilibrium position of germanium atoms is cubic $4\bar{3}m$, with the inclusion of only the dipole-dipole component of resonant scattering, the structural amplitude of such reflections also vanishes. The spectrum of such a reflection was measured in several SR sources and was initially described as a result of dipole-quadrupole resonant scattering [26]. However, this assumption could not explain the increase in the intensity of purely resonant Bragg reflections Ge(002) and Ge(006): these appeared with increasing temperature at an incident radiation energy near the *K*-absorption edge, which was first experimentally observed in Ref. [56]. This behavior of intensity is anomalous, since the intensity of allowed reflections decreases with increasing temperature, which is described by the Debye–Waller factor [16, 57].

To describe this phenomenon, a model was proposed in [30], in which an assumption was made about the existence, apart from dipole-quadrupole scattering, of an additional resonance component of the atomic scattering factor caused by a decrease in the symmetry of the instantaneous positions of germanium atoms due to thermal vibrations. The interference of the two specified SR scattering channels is not strongly manifested in the spectral shape of forbidden reflections, and their separation turned out to be possible due to the influence of an external factor: temperature. Its variation changes greatly the ratio of the magnitude of the two contributions to the intensity of the diffraction reflection. A comparison with this theory made it possible to explain the experimental results for germanium in a wide temperature range [35, 56].

A significantly different effect arises from the interference of the dipole-quadrupole and thermally induced scattering channels in forbidden reflections observed in ZnO and GaN crystals with a wurtzite structure [36, 58, 59] near the *K*-absorption edges of zinc and gallium, respectively. Similar to the case of germanium crystals, they have two channels of resonant scattering. However, the interference of these channels entails a significant rearrangement of the Zn(115) and GaN(115) forbidden reflection spectra with temperature (Fig. 1a).

One can see from Fig. 1a that the spectral shape of the ZnO(115) reflection changes markedly with temperature. To explain this effect, a model of one low-lying optical mode was proposed. According to this model, the structural factor of the forbidden diffraction reflection can be represented as a linear combination of a temperature-independent (dipole-quadrupole) and a temperature-dependent (thermally induced) component. Such a simplified model, by and large, made it possible to describe the observed phenomenon. To clarify the resultant data, an *ab initio* simulation of the phonon vibration modes and displacement correlations of zinc and oxygen atoms in *w*-ZnO was performed. Comparing the results of quantum mechanical simulations and a simplified approach, which took into account one low-lying vibration mode, showed that the results are hardly different at high temperatures, but differ at temperatures below about 600 K (Fig. 1b). The difference can be attributed to the fact that higher-frequency optical vibration modes should also be taken into account at low temperatures.

An even more interesting case is related to the existence of three channels of resonant SR scattering in RDP (RbH_2PO_4) and KDP (KH_2PO_4) crystals [60, 61]. Observed In these studies was a jump in the intensity of forbidden diffraction reflections near the *K*-absorption edge of rubidium and potassium, respectively, which was caused by the removal of the prohibition on dipole-dipole resonant SR scattering in the para- to ferroelectric phase transition. However, not only do the spectra rearrange with temperature in the paraelectric phase, but they also develop a strong azimuthal dependence. Figure 2a shows the reflection spectra of KDP(222) at several temperature values at an azimuthal angle of 62°. To describe the effects observed, in addition to the dipole-quadrupole and thermally induced components of resonant SR scattering, introduced into consideration was another physical mechanism related to the symmetry of instantaneous proton configurations randomly filling only half of the crystallographic position. In the proposed model, such configurations were considered point defects that distort the local atomic structure and cause additional anisotropy of the atomic

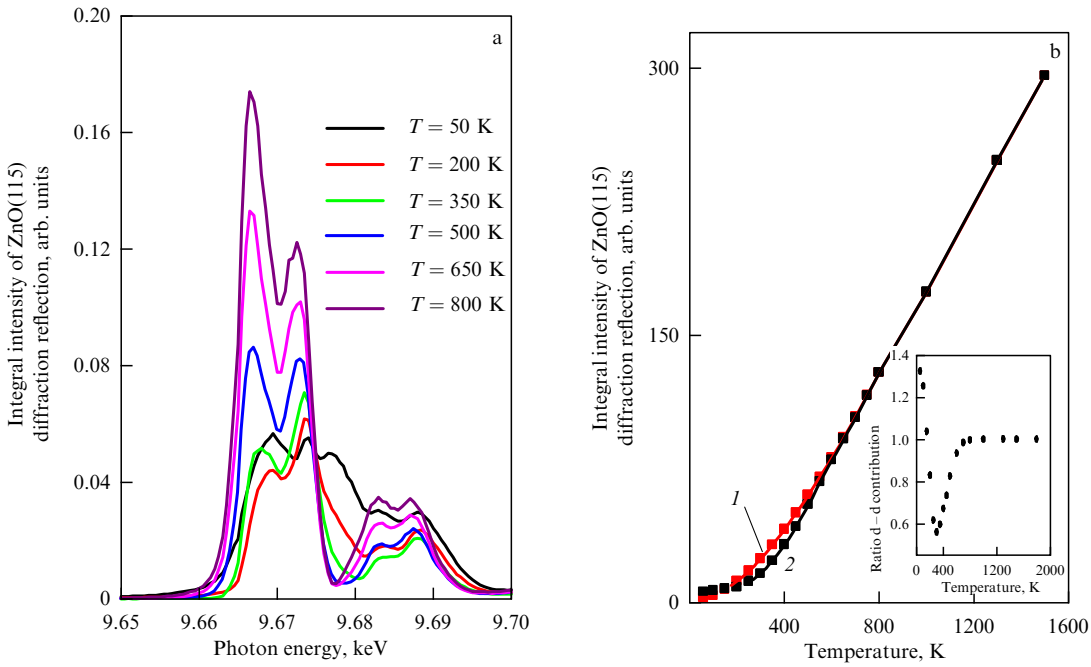

Figure 1. (a) Experimental temperature dependences of angle-integrated intensity spectra of forbidden ZnO(115) Bragg diffraction reflection near *K*-absorption edge of zinc ($E_{\text{Zn }K\text{-edge}} = 9.659$ keV) [59, 34]. (b) Temperature dependence of intensity of ZnO(115) forbidden diffraction reflection integrated over incident radiation energy. *1* — single-mode model, *2* — *ab initio* simulations. Inset shows intensity ratio of thermally induced components simulated *ab initio* and in single-mode model.

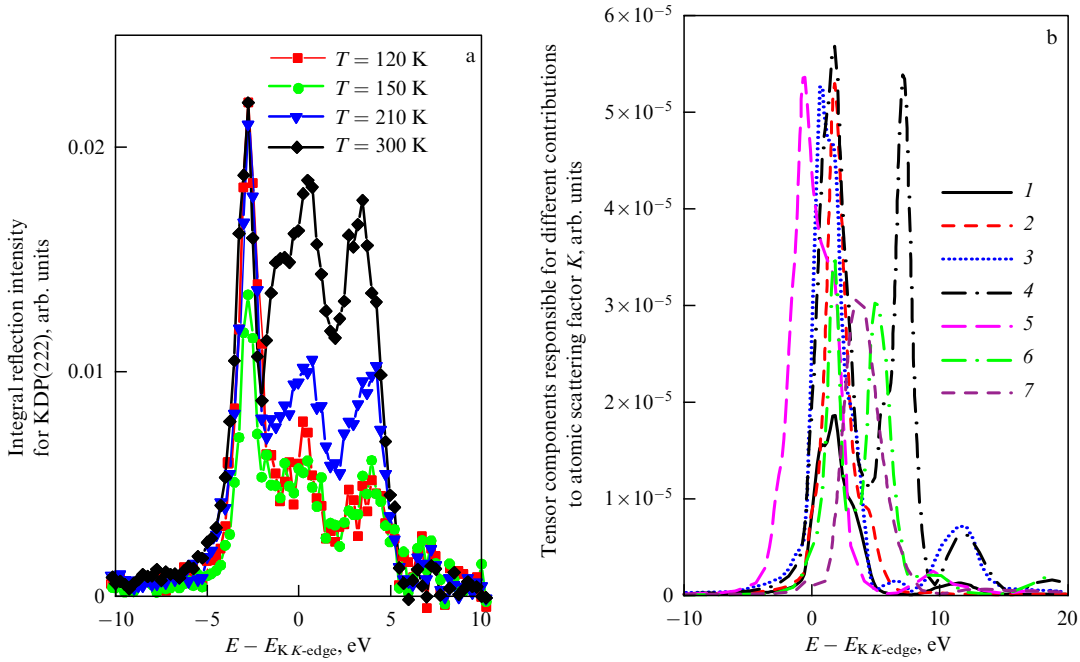

Figure 2. (a) Experimental temperature dependences of angle-integrated intensity spectra of forbidden Bragg diffraction reflection of KDP(222) near potassium absorption edge ($E_{\text{K }K\text{-edge}} = 3.608$ keV) at an azimuthal angle of 62° [34, 59]. (b) Model spectral dependences of squares of moduli of tensor coefficients that enter in various resonance contributions to KDP(222) reflection: *1* — dipole-quadrupole $|f_{xxz}^{\text{dq}}|^2$, *2* — dipole-quadrupole $|f_{zxx}^{\text{dq}}|^2$, *3* — thermally induced $|f_{xx}^{\text{TMI}}|^2$, *4* — due to instantaneous polar configuration of protons $|f_{xx}^{\text{ht, polar}}|^2$, *5* — thermally induced $|f_{xz}^{\text{TMI}}|^2$, *6* — due to instantaneous configuration of protons according to Slater $|f_{xz}^{\text{ht, slater}}|^2$, *7* — due to instantaneous configuration of protons according to Takagi $|f_{xz}^{\text{ht, takagi}}|^2$.

factors of the surrounding atoms, with the result that the resonant structural amplitude assumes the form

$$F_{\alpha\beta} = a^{\text{dq}} F_{\alpha\beta}^{\text{dq}} + a^{\text{TMI}} F_{\alpha\beta}^{\text{TMI}} + \sum_X a^X F_{\alpha\beta}^X , \qquad (5)$$

where the summation is performed over all the most probable proton configurations, and a^i are the temperature-dependent partial mixing coefficients of the different components. Each of these components has its own spectral dependence, but the reflection intensity at each temperature is determined by the interference of radiation caused by three scattering channels, with the inclusion of the mixing coefficients. Figure 2b shows the calculated spectral dependences of the squares of the moduli of the tensor coefficients, which enter in the various resonance contributions. They mix differently at different temperatures, which entails variations in the KDP(222) reflection spectrum.

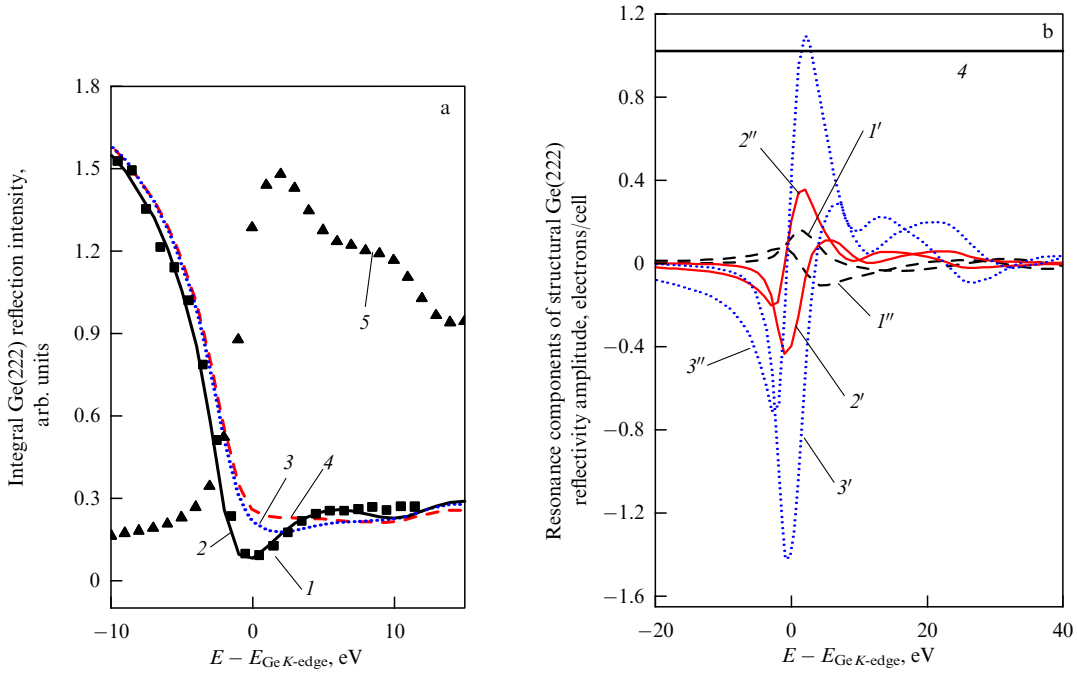

Figure 3. (a) Spectrum of angle-integrated intensity of Ge(222) diffraction reflection near *K*-absorption edge of germanium ($E_{\text{Ge }K\text{-edge}} = 11.103$ keV): *1* — experimental data; *2* — calculation with inclusion of dipole-quadrupole and thermally induced resonant components; *3* — calculation ignoring resonant components; *4* — calculation including only dipole-quadrupole component, *5* — absorption spectrum. (b) Spectrum of structural amplitude of Ge(222)diffraction reflection: *1′* and *1″* — real and imaginary parts of dipole-quadrupole component of resonant structural amplitude; *2′* and *2″* — real and imaginary parts of total resonant structural amplitude; *3′* and *3″* — real and imaginary parts of total resonant structural amplitude at temperature of 700 K (calculation); *4* — nonresonant component of structural amplitude.

Proceeding from the resultant temperature dependences of these coefficients, it was proved that, as expected, the dipole-quadrupole scattering component was temperature independent. The thermally induced dipole-dipole component was described within the framework of one optical vibration mode with an energy of 32 meV, and the dipole-dipole components caused by instantaneous proton configurations were described within the framework of the Arrhenius law with the activation energy of polar configurations of 18.6 ± 0.5 meV and with the activation energy of the most energetically favorable Slater-type configurations of 7.3 ± 0.2 meV. This is in reasonable agreement with other existing experimental data (the geometry of both configuration types is described at length in Ref. [37].

Similar studies are being actively pursued for various materials at present and will undoubtedly continue in the near future. For instance, it has recently been proposed in [62, 63] to use the interference between charge and magnetic resonance contributions to the diffraction of circularly polarized SR to study RuO_2 crystals, which are popular candidates for so-called altermagnetics [64]. Interference makes it possible to analyze fine details of magnetic ordering that are inaccessible to magnetic neutron diffraction. Forbidden diffraction reflections in RuO_2 have been reported earlier in several papers [65, 66], and their detailed study using circularly polarized SR will allow us to advance our understanding of the physics of altermagnetism.

4. Interference of nonresonance and resonance X-ray scattering channels

To understand the physics of resonance SR scattering, it is necessary to know not only the absolute value, but also the phase of the resonant part of the atomic scattering amplitude. In the examples discussed in Section 3, it is possible to find only the ratio between different contributions to the resonant atomic amplitude, while their absolute value can only be found by analyzing the spectral dependence of the resonant diffraction Bragg reflection produced by the interference of the resonant and known nonresonant scattering channels. This approach was first used in Ref. [67] for the experimental determination of the absolute value and phase of the resonance component of the atomic scattering factor of iron in pyrite FeS_2 from the interference pattern of the resonant and multi-wave nonresonant scattering channels.

In Ref. [68], the spectral dependence of the absolute value and phase of the resonant component of the atomic scattering factor is determined from the interference of the resonant and nonresonant channels of the (222) diffraction reflection in a germanium crystal near the *K*-absorption edge of germanium. This reflection is forbidden by the particular extinction rules of the $Fd\bar{3}m$ space group but is allowed by the general ones. Therefore, even in the nonresonant region, it is marginally allowed due to the asymmetry of the electron atomic density and the anharmonicity of atomic vibrations [69, 70]. The nonresonant Ge(222) structural reflectivity factor at room temperature is known and is $F^{(\text{nr})}(222) = +1.02$ electron/unit cell [69], i.e., the nonresonant component of the atomic scattering factor is approximately 0.128 electron/atom.

An experiment to observe the Ge(222) Bragg diffraction reflection near the *K*-absorption edge at room temperature was performed at the Kurchatov synchrotron radiation source (Fig. 3a).

If the resonance component of the atomic scattering factor were absent, the shape of the intensity spectrum of the $I^{(\text{nr})}(222)$ diffraction reflection in the kinematic approximation would be determined only by the type of absorption

spectrum, which is isotropic in a cubic crystal, which allows a simplified expression to be used instead of expression (3):

$$I^{(\mathrm{nr})}(222) \sim \frac{\left|F^{(\mathrm{nr})}(222)\right|^2}{\mu(E)}\,, \qquad (6)$$

where $\mu(E)$ is the absorption coefficient, which increases sharply near the absorption edge. As one can see from Fig. 3, the greatest difference between the experimental data obtained and the model spectrum $I^{(\mathrm{nr})}(222)$ is observed precisely in the vicinity of the absorption edge.

As shown in Section 3, the atomic scattering factor in the vicinity of the absorption edge must take into account the tensor resonance part, which includes the temperature-independent dipole-quadrupole (dq) and temperature-dependent thermally induced (TMI) components [56]. So, the intensity of the Ge(222) diffraction reflection can be represented as

$$I(222) \sim \frac{\left|F^{(\mathrm{nr})}(222)\delta_{jk} + F_{jk}^{\mathrm{TMI}}(222) + F_{jk}^{\mathrm{dq}}(222)\right|^2}{\mu(E)}\,. \qquad (7)$$

Direct simulations of the diffraction reflection intensity made it possible to determine the amplitude and phase of the resonant structural amplitude, as well as to show the destructive interference of the dipole-quadrupole and thermally induced scattering channels.

Figure 3b shows the calculated real and imaginary parts of the total resonant structural amplitude of the Ge(222) diffraction reflection at 700 K. One can see that the magnitude of the resonant structural amplitude increases with temperature (curves *3′* and *3″*), and for 700 K at some energies it may exceed the nonresonant structural amplitude of the Ge(222) diffraction reflection (line *4*). High temperatures, at which the nonresonant and resonant structural amplitudes are comparable, would be the most optimal ones for observing their interference.

5. Resonance scattering of synchrotron radiation by crystals with atoms residing in nonequivalent crystallographic sites

Atoms of one chemical element may occupy several crystallographic positions in crystals. In this case, the symmetry of the local environment and, consequently, the resonance components of the atomic scattering factor of atoms of one element located in different positions may differ from each other.

The limiting case of such crystals are incommensurately modulated structures, where all atoms of one element are, generally speaking, nonequivalent [71] and have different scattering factors. This, in particular, may lead to the appearance of additional satellites in the diffraction reflection spectra at radiation energies close to the absorption edges of the atoms of the structure [72]. A simpler case is realized when atoms of one type occupy two nonequivalent positions. But, even in this case, curious effects arise in the spectra of forbidden diffraction reflections caused by the interference of radiation scattered by atoms in different positions. One of the first experimental studies of this type was that of (300), (500) and (700) forbidden reflections near the iron *K*-absorption edge in iron orthoborate Fe_3BO_6 [73]. The first two diffraction reflections correspond to the constructive interference of dipole-dipole scattering by iron atoms in positions 4(*b*) and 8(*d*) of the *Pnma* space group, whereas in the (700) reflection

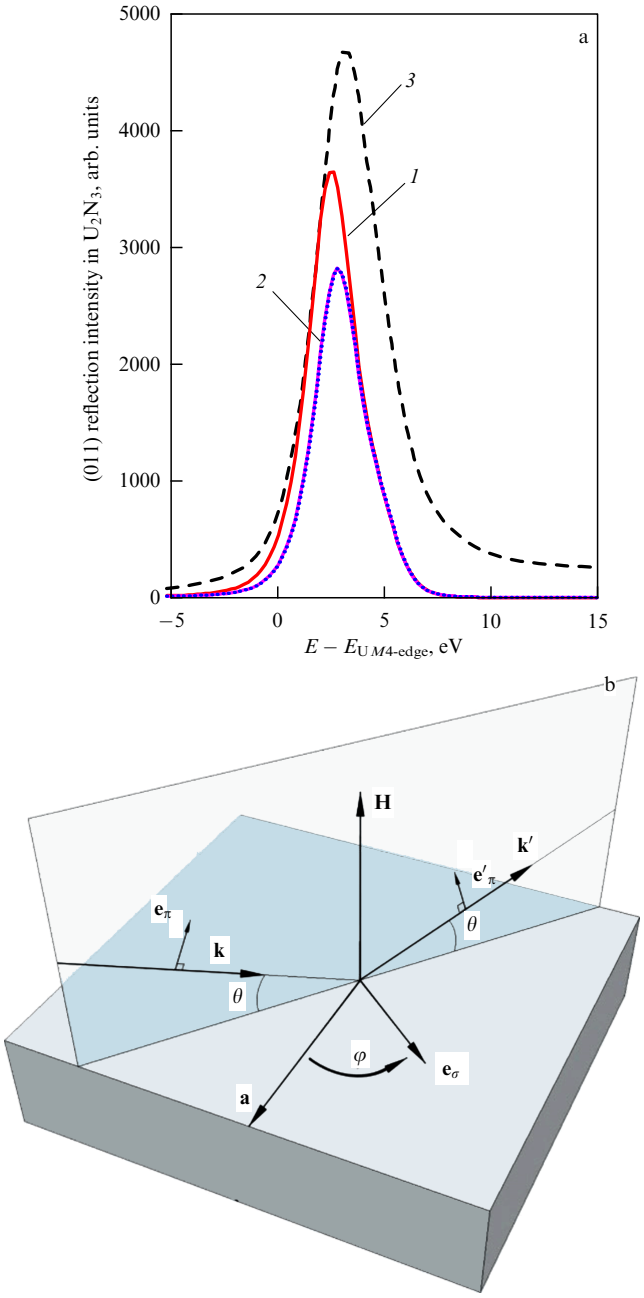

Figure 4. (a) Model spectrum of integral intensity of (011) forbidden diffraction reflection in U_2N_3 crystal near M_4-absorption edge of uranium ($E_{\mathrm{U}\,M_4\text{-edge}} = 3.728$ eV): *1* — azimuthal angle: 0°; *2* — azimuthal angle: 180°; *3* — absorption spectrum. (b) Experiment geometry demonstrating orientation of incident radiation wave vectors **k** with polarization **e** and scattered radiation **k′** with polarization **e′** relative to the crystal. **H** — reciprocal lattice vector, **a** — one of the crystal axes, θ — Bragg angle, φ — azimuthal angle.

the interference is destructive, with the result that it is weak. A very interesting shape in the pre-edge region is exhibited by the spectrum of the azimuthal dependence of the (300) reflection caused by the interference of the radiation corresponding to the dipole-quadrupole and quadrupole-quadrupole channels of resonance scattering of SR from two crystallographically nonequivalent positions of iron atoms. However, in the region of the main peak, where the dipole-dipole component of the structural factor prevails, the interference of the radiation scattered by iron atoms in both

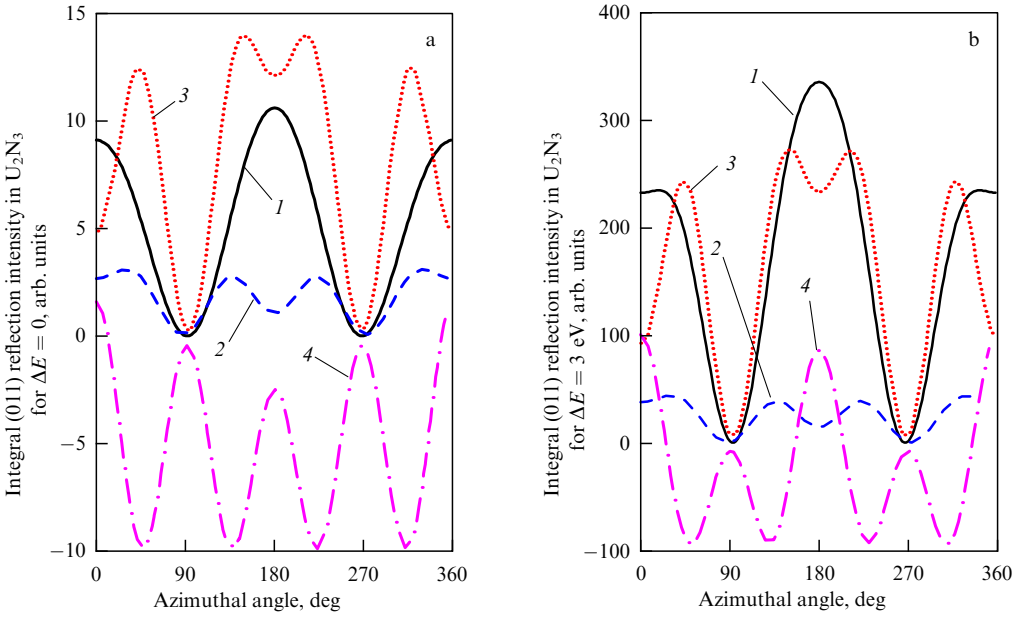

Figure 5. Model azimuthal dependences of integral intensity of (011) diffraction reflection in U_2N_3 crystal at an incident radiation energy corresponding to M_4-absorption edge of uranium (a) and to a 3 eV deviation from M_4-absorption edge of uranium (b): *1* — reflection intensity if positions of uranium atom existed separately; *2* — reflection intensity corresponding to uranium atom in first position; *3* — reflection intensity corresponding to uranium atom in second position; *4* — intensity of interference term.

positions is weakly manifested in the azimuthal dependence of the intensity.

A completely different situation is realized in the U_2N_3 crystal in the course of SR diffraction with an energy close to the M_4-absorption edge of uranium ($E_{\mathrm{U}\ M_4\text{-edge}} = 3.728$ keV) [74]. In this compound with $Ia\bar{3}$ symmetry, the uranium atoms occupy two crystallographically nonequivalent positions. The $U1$ atoms are in position $8(b)$ with local $\bar{3}$ symmetry, and the $U2$ atoms are in position $24d$ and lie on the two-fold symmetry axes. The difference in the symmetry of the uranium-atom positions entails a difference in the tensor components of the resonance atomic factors determining the properties of the Bragg reflections. In this work, the spectra of several Bragg reflections were measured, among which (105) and (015) are forbidden. The results obtained show that the spectral and azimuthal dependences of the forbidden reflections arise from dipole-dipole resonance transitions in uranium atoms and result from the existence of ordering of quadrupole moments. Figure 4a shows the results of simulations of the diffraction (011) reflection spectra using the FDMNES program for two values of the azimuthal angle φ, which describes crystal rotation relative to the scattering plane (Fig. 4b). The dotted absorption spectrum of uranium is depicted to show the position of the forbidden reflection on the energy scale. One can see that the (011) reflection spectra depend on the value of the angle φ, and this is a consequence of interference of the radiation scattered by uranium atoms in two nonequivalent positions. However, there is no substantial change in the shape of the diffraction reflection spectrum versus the azimuthal angle as, for example, in KDP.

Interference phenomena in this crystal are much more pronounced in the azimuthal dependence of the intensity of diffraction reflection. In order to trace the effect of interference of radiation scattered by two nonequivalent positions of uranium atoms, we represent the intensity of reflections as a sum of three components: two of them are proportional to the square of the structural amplitude, which corresponds to each of the uranium positions separately, but there is also an additional component $I_{\mathrm{int}}(E)$ caused by the interference of radiation scattered by atoms in two different positions:

$$I(0kl) = \left|F(U1,E) + F(U2,E)\right|^2 = \left|F(U1,E)\right|^2 + \left|F(U2,E)\right|^2 + I_{\mathrm{int}}(E)\,. \qquad (8)$$

The last expression implies averaging over the polarization of scattered radiation, since this polarization is commonly not measured. Figure 5 shows the azimuthal intensities of the (011) diffraction reflection, as well as of all three components of the forbidden reflection intensity for two values of the incident radiation energy. It is evident that the total intensity of the diffraction reflection is not the sum of the intensities that would correspond to such a reflection were the uranium positions existing separately. Furthermore, in different domains of azimuthal angles, the interference term has different signs, which results in both an increase and a decrease in the total intensity.

Careful measurements of the azimuthal dependences of several forbidden reflections in this compound, augmented with polarization measurements, will allow in the future separating the resonance contributions to the scattering from uranium atoms in two positions and resolving the controversial issue [75] about the existence of ordering of quadrupoles on uranium atoms in the $8(b)$ position. Therefore, the study of this interesting $5f$ compound with an intricate crystalline, electronic, and magnetic structure is still in its infancy. Notably, at low temperatures in the U_2N_3 crystal near the M_4 edge, purely magnetic diffraction reflections (003) were also observed [76], but the details of the magnetic structure have yet to be studied.

6. Conclusions

So, the study of interference phenomena in X-ray diffraction spectroscopy allows us to advance significantly in understanding the physical state of atoms in crystals, as well as to distinguish even the states of atoms of one element located in different crystallographic positions. Numerous examples of such research performed recently and presented in this paper show their informativeness and importance for further progress in this area of science.

Acknowledgments. This research was carried out within the framework of the state assignment of M.V. Lomonosov Moscow State University. The work of V.E. Dmitrienko was performed within the framework of the state assignment of the National Research Center Kurchatov Institute.

The authors express their appreciation to V.A. Bushuev, M.V. Gorkunov, and E.Kh. Mukhamedzhanov for their helpful advice and critical comments.

References

1. Mittemeijer E J, Welzel U (Eds) *Modern Diffraction Methods* (Weinheim: Wiley-VCH, 2013)
2. Lee P A et al. *Rev. Mod. Phys.* **53** 769 (1981)
3. Borovskii I B et al. *Sov. Phys. Usp.* **29** 539 (1986); *Usp. Fiz. Nauk* **149** 275 (1986)
4. Rehr J J, Albers R C *Rev. Mod. Phys.* **72** 621 (2000)
5. Hodeau J-L et al. *Chem. Rev.* **101** 1843 (2001)
6. Kochubey D I, Kanazhevskiy V V *Chem. Sustainable Development* (1) 13 (2013); *Khim. Interesakh Ustoichivogo Razvitiya* (1) 21 (2013)
7. Bulou H et al. (Eds) *Magnetism and Accelerator-Based Light Sources. Proc. of the 7th Intern. School Synchrotron Radiation and Magnetism, Mittelwihr, France, 2018* (Springer Proc. in Physics, Vol. 262) (Cham: Springer, 2021) https://doi.org/10.1007/978-3-030-64623-3
8. Van Bokhoven J A, Lamberti C *X-Ray Absorption and X-Ray Emission Spectroscopy*: *Theory and Applications* (Hoboken, NJ: John Wiley and Sons, 2016)
9. Jaeschke E J et al. (Eds) *Synchrotron Light Sources and Free-Electron Lasers. Accelerator Physics, Instrumentation and Science Applications* (Cham: Springer, 2020) https://doi.org/10.1007/978-3-030-23201-6
10. Murakami Y et al. *Phys. Rev. Lett.* **80** 1932 (1998)
11. Wilkins S B et al. *Phys. Rev. B* **71** 245102 (2005)
12. Collins S P et al. *J. Phys. Condens. Matter* **19** 213201 (2007)
13. Smekhova A et al. *Soft Matter* **18** 89 (2022)
14. Caciuffo R, Lander G H, van der Laan G *Rev. Mod. Phys.* **95** 015001 (2023)
15. Aroyo M I (Ed.) *International Tables for Crystallography* Vol. A (Weinheim: Wiley-VCH, 2016) https://doi.org/10.1107/9780955360206000114
16. James R W *The Crystalline State* Vol. 2 *The Optical Principles of the Diffraction of X-Rays* (Eds Sir W H Bragg, W L Bragg) (London: G. Bell and Sons, 1948); Translated into Russian: *Opticheskie Printsipy Diffraktsii Rentgenovskikh Luchei* (Kristallicheskoe Sostoyanie (Crystalline State), Vol. 2) (Moscow: IL,1950)
17. Mark H, Szilard L *Z. Phys.* **33** 688 (1925)
18. Kolpakov A V, Bushuev V A, Kuz'min R N *Sov. Phys. Usp.* **21** 959 (1978); *Usp. Fiz. Nauk* **126** 479 (1978)
19. Zhizhimov O L, Khriplovich I B *Sov. Phys. JETP* **60** 313 (1984); *Zh. Eksp. Teor. Fiz.* **87** 547 (1984)
20. Blume M *J. App. Phys.* **57** 3615 (1985)
21. Hannon J P et al. *Phys. Rev. Lett.* **61** 1245 (1988)
22. Kirfel A, Petcov A, Eichhorn K *Acta Cryst. A* **47** 180 (1991)
23. Altarelli M, in *Magnetism and Synchrotron Radiation*: *Towards the Fourth Generation Light Sources* (Springer Proc. in Physics, Vol. 151, Eds E Beaurepaire et al.) (Cham: Springer, 2013) p. 95, https://doi.org/10.1007/978-3-319-03032-6_3
24. Belyakov V A, Dmitrienko V E *Sov. Phys. Usp.* **32** 697 (1989); *Usp. Fiz. Nauk* **158** 679 (1989)
25. Brouder C *J. Phys. Condens. Matter* **2** 701 (1990)
26. Templeton D H, Templeton L K *Phys. Rev. B* **49** 14850 (1994)
27. Carra P, Thole B T *Rev. Mod. Phys.* **66** 1509 (1994)
28. Dmitrienko V E, Ovchinnikova E N *Acta Cryst. A* **57** 642 (2001)
29. Di Matteo S et al. *Phys. Rev. Lett.* **91** 257402 (2003)
30. Dmitrienko V E, Ovchinnikova E N, Ishida K *JETP Lett.* **69** 938 (1999); *Pis'ma Zh. Eksp. Teor Fiz.* **69** 885 (1999)
31. Dmitrienko V E *Acta Cryst. A* **39** 29 (1983)
32. Templeton D H, Templeton L K *Acta Cryst. A* **41** 365 (1985)
33. Dmitrienko V E et al. *Acta Cryst. A* **61** 481 (2005)
34. Dmitrienko V E, Ovchinnikova E N *Acta Cryst. A* **56** 340 (2000)
35. Kirfel A, Grybos J, Dmitrienko V E *Phys. Rev. B* **66** 165202 (2002)
36. Oreshko A P et al. *J. Phys. Condens. Matter* **24** 245403 (2012)
37. Beutier G et al. *Phys. Rev. B* **92** 214116 (2015)
38. Dmitrienko V E et al. *Nature Phys.* **10** 202 (2014)
39. Beutier G et al. *Phys. Rev. Lett.* **119** 167201 (2017)
40. Dmitrienko V E et al. *JETP Lett.* **92** 383 (2010); *Pis'ma Zh. Eksp. Teor. Fiz.* **92** 424 (2010)
41. Pincini D et al. *Phys. Rev. B* **98** 104424 (2018)
42. Oreshko A P, Ovchinnikova E N, Dmitrienko V E *Crystallogr. Rep.* **68** 351 (2023); *Kristallografiya* **68** 346 (2023)
43. Richter C et al. *Nat. Commun.* **9** 178 (2018)
44. Ovchinnikova E N et al. *JETP Lett.* **110** 568 (2019); *Pis'ma Zh. Eksp. Teor. Fiz.* **110** 563 (2019)
45. Blume M, in *Resonant Anomalous X-Ray Scattering* (Eds G Materlik, C J Sparks, K Fisher) (Amsterdam: Elsevier, 1994) p. 495
46. Joly Y et al. *Phys. Rev. B* **86** 220101 (2012)
47. Lovesey S W, Collins S P *J. Synchrotron Rad.* **8** 1065 (2001)
48. Collins S P et al. *J. Phys. Conf. Ser.* **425** 132015 (2013)
49. Oreshko A P *Moscow Univ. Phys. Bull.* **76** 187 (2021); *Vestn. Mosk. Univ. Ser. 3. Fiz. Astron.* (4) 3 (2021)
50. Rehr J J et al. *Phys. Chem. Chem. Phys.* **12** 5503 (2010)
51. Blaha P et al. *J. Chem. Phys.* **152** 074101 (2020)
52. Bunău O, Joly Y *J. Phys. Condens. Matter* **21** 345501 (2009)
53. Chang S-L *Multiple Diffraction of X-Rays in Crystals* (Berlin: Springer-Verlag, 1984); Translated into Russian: *Mnogovolnovaya Difraktsiya Rentgenovskikh Luchei v Kristallakh* (Moscow: Mir, 1987)
54. Kozlovskaya K et al. *Crystals* **11** 1389 (2021)
55. Ji S et al. *Phys. Rev. Lett.* **91** 257205 (2003)
56. Kokubun J et al. *Phys. Rev. B* **64** 073203 (2001)
57. Iveronova V I, Revkevich G P *Teoriya Rasseyaniya Rentgenovskikh Luchei* (X-Ray Scattering Theory) (Moscow: Izd. MGU, 1978)
58. Collins S P et al. *Phys. Rev. B* **68** 064110 (2003)
59. Beutier G et al. *Eur. Phys. J. Special Topics* **208** 53 (2012)
60. Richter C et al. *Phys. Rev. B* **89** 094110 (2014)
61. Beutier G et al. *J. Phys. Conf. Ser.* **519** 012006 (2014)
62. Lovesey S W, Khalyavin D D, van der Laan G *Phys. Rev. B* **105** 014403 (2022)
63. Lovesey S W, Khalyavin D D, van der Laan G *Phys. Rev. B* **108** L121103 (2023)
64. Ohldag H *npj Spintronics* **2** 57 (2024)
65. Zhu Z H et al. *Phys. Rev. Lett.* **122** 017202 (2019)
66. Gregory B Z et al. *Phys. Rev. B* **106** 195135 (2022)
67. Kokubun J et al. *Phys. Rev. B* **69** 245103 (2004)
68. Mukhamedzhanov E Kh et al. *JETP Lett.* **86** 783 (2008); *Pis'ma Zh. Eksp. Teor. Fiz.* **86** 896 (2007)
69. Roberto J R, Batterman B W, Keating D T *Phys. Rev. B* **9** 2590 (1974)
70. Tischler J Z, Batterman B W *Phys. Rev. B* **30** 7060 (1984)
71. Ovchinnikova E N, Dmitrienko V E *Acta Cryst. A* **55** 20 (1999)
72. Bindi L et al. *Crystallogr. Rep.* **51** 941 (2006); *Kristallografiya* **51** 1006 (2006)
73. Beutier G et al. *J. Phys. Condens. Matter* **21** 265402 (2009)
74. Lawrence Bright E et al. *Phys. Rev. B* **110** 125138 (2024)
75. Lovesey S W *Phys. Rev. B* **108** 235151 (2023)
76. Lawrence Bright E et al. *Phys. Rev. B* **100** 134426 (2019)